

Effect of H₂SO₄ addition on the corrosion behaviour of AISI 304 austenitic stainless steel in methanol-HCl solution

V.B. Singh* and Monali Ray

Department of Chemistry, Banaras Hindu University, Varanasi - 221005, India

*E-mail: vijaybs@bhu.ac.in

Received: 23 December 2006 / Accepted: 20 March 2007 / Published: 1 April 2007

Effect of sulphuric acid addition on the corrosion behaviour of AISI 304 austenitic stainless steel was investigated in different concentrations of HCl (0.001 – 1.0 M) in methanol using potentiostatic polarization, cyclic anodic polarization and open-circuit potential (OCP) measurements. In methanol-HCl solution, only active anodic dissolution occurred and the rate of corrosion increased with concentration of HCl. Scanning electron microscopic studies revealed grain boundary attack of the specimen. The addition of H₂SO₄ into methanol-HCl solutions with H₂SO₄ to HCl concentration ratio $\geq 10:1$ stimulated the dissolution rate in the active region, but at higher potentials, facilitated passivation with occurrence of pitting on the steel surface. Increase in H₂SO₄ concentration enhanced passivity by broadening the range of passivity and making the pitting potential (E_{pit}) and the protection potentials (E_{prot}) nobler due to higher inherent water content of H₂SO₄. Simultaneously, the passivation current density (i_p) also increased indicating the formation of a more defective passive film probably due to higher acidity of the solution.

Keywords: AISI 304 stainless steel; Corrosion; Passivity; Methanol; Scanning electron microscopy

1. INTRODUCTION

Acidic solutions of hydrochloride acid and sulphuric acid have wide industrial applications, the most important fields being acid pickling, acid descaling, industrial cleaning and oil-well acidizing. In aqueous solutions of acids, the surface of metals and alloys are covered with highly protective oxyhydroxide passive film. However, in non-aqueous solutions, it is strongly dependent on the water content of the solutions. Investigation conducted on iron, chromium and nickel in anhydrous sulphuric acid solution shows that the molar ratio of acid to water has to be less than 1:4 for the formation of passive oxide-hydroxide film [1]. In anhydrous methanolic solution of sulphuric acid, the passivity of

stainless steel was also due to the water content of sulphuric acid [2]. Several other studies performed on different metals have shown that in concentrated anhydrous solution of sulphuric acid, passivation proceeds with the participation of undissociated acid molecules, whereas in dilute solutions ($M < 6$), water molecules are the main passivating agents [3, 4].

In the present investigation, methanol was chosen as the electrolytic medium keeping in view its increasing importance as a source of hydrogen in fuel cells. Methanol generally contains low levels of acid, chloride and sulphates as impurities. Therefore, the present work aims at investigating the corrosion behaviour of AISI 304 austenitic stainless steel in methanolic solution of hydrochloric acid and the effect of addition of sulphuric acid into it.

2. EXPERIMENTAL

The specimen for the present investigation was the commercial AISI 304 austenitic stainless steel (Good Fellow, UK) having chemical composition as follows: 18.0% Cr, 10.0% Ni, 2.0% Mn, 0.08% C, 0.03% S, 1.0% Si and balanced iron. The samples were polished mechanically to a mirror finish using successive grades of emery papers followed by polishing with alumina powder. Then the specimens were washed thoroughly with bidistilled water, degreased with acetone and transferred quickly into the electrochemical cell.

The cell used was a conventional three electrode electrochemical cell consisting of a working electrode (sample), a platinum counter electrode of large surface area and a saturated calomel reference electrode (SCE). Details of experimental set up and working procedures were described elsewhere [5].

The electrochemical polarization experiments were carried out using a potentiostat (Wenking POS 73). The working electrode specimen of 2 cm^2 exposed area was immersed in the experimental solution for two hours to stabilize the open circuit potential (OCP). The polarization was performed potentiostatically by starting at a negative potential and then moving to the positive direction in steps of 20 mV/min. For the precise determination of pitting potential (E_{pit}) and protection potential (E_{prot}), cyclic anodic polarization and current verses time transients were recorded using X-Y recorder 2000 (Houston Instruments) at a scan rate of 1 mV/sec. All measurements were carried out at $35 \pm 1^\circ \text{C}$ under unstirred conditions in aerated solutions. The solutions were prepared using distilled purified methanol and analytical grades of chemicals (HCl, H_2SO_4). After the electrochemical studies, the specimens were rinsed in deionised water in an ultrasonic bath and were subsequently examined by scanning electron microscopy (Philips XL-20). Spectral analysis of the experimental solutions after the polarization measurements was performed by CARY 2390 spectrophotometer.

3. RESULTS AND DISCUSSION

3.1. Open-circuit measurements

The open-circuit potential (OCP) of AISI 304 austenitic stainless steel in methanolic solution containing different concentrations of HCl (0.001 – 1.0 M) was recorded over two hours (Figure 1[a]). The potential took about 60 min to reach the steady-state value except in 1.0 M. Also, as the

concentration of hydrochloric acid increased, the steady-state potential shifted towards more negative values indicating the increased corrosion susceptibility of the steel. Similar results have been reported earlier for Cu-Ni alloys in aqueous chloride solutions [6].

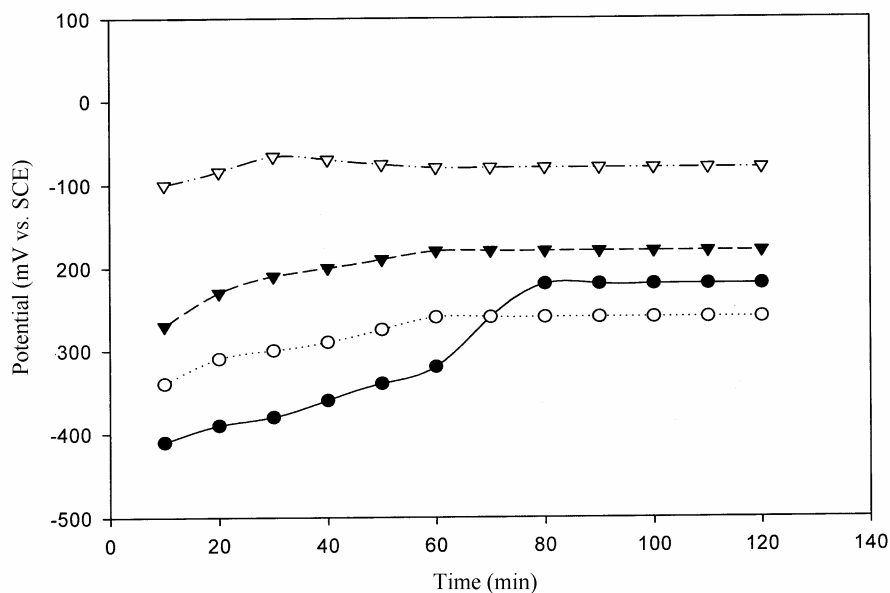


Figure 1(a). OCP vs. time curve of AISI 304 austenitic stainless steel in different concentrations of HCl in methanol at 35°C. (i) ∇ 0.001 M HCl, (ii) \blacktriangledown 0.01 M HCl, (iii) \circ 0.1 M HCl, (iv) \bullet 1.0 M HCl

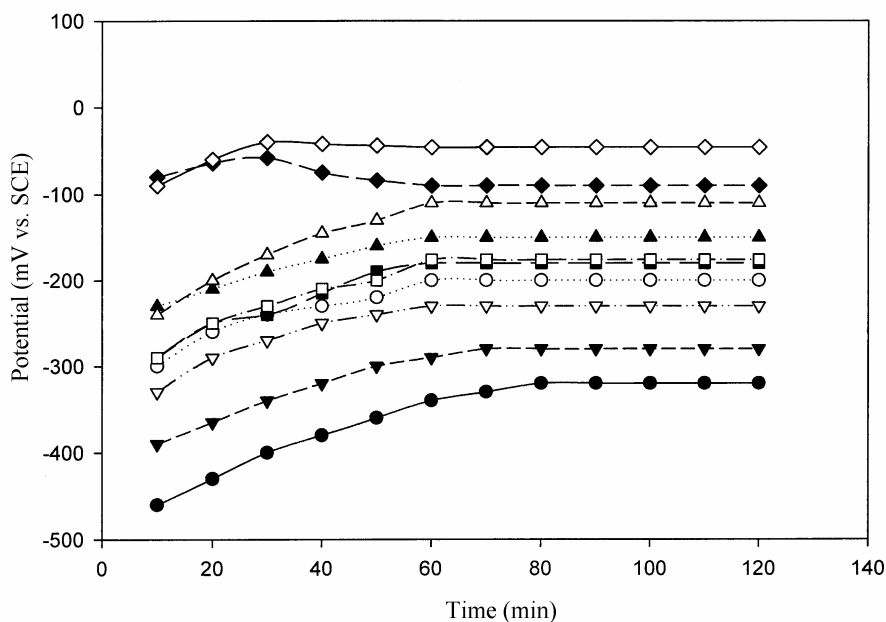


Figure 1(b). OCP vs. time curve of AISI 304 austenitic stainless steel in different composition mixtures of HCl and H_2SO_4 in methanol at 35°C. (i) Δ 0.001 M HCl + 0.001 M H_2SO_4 , (ii) \blacktriangle 0.001 M HCl + 0.01 M H_2SO_4 , (iii) \triangle 0.001 M HCl + 0.1 M H_2SO_4 , (iv) \blacklozenge 0.001 M HCl + 1.0 M H_2SO_4 , (v) \square 0.01 M HCl + 0.01 M H_2SO_4 , (vi) \blacksquare 0.01 M HCl + 0.1 M H_2SO_4 , (vii) ∇ 0.01 M HCl + 1.0 M H_2SO_4 , (viii) \blacktriangledown 0.1 M HCl + 0.1 M H_2SO_4 , (ix) \circ 0.1 M HCl + 1.0 M H_2SO_4 , (x) \bullet 1.0 M HCl + 1.0 M H_2SO_4

Similar experiments were performed in mixture solutions of hydrochloric acid and sulphuric acid of varying concentration ratio. The concentration ranges were 1.0 M HCl + 1.0 M H₂SO₄, 0.1 M HCl + (0.1 – 1.0) M H₂SO₄, 0.01 M HCl + (0.01 – 1.0) M H₂SO₄ and 0.001 M HCl + (0.001 – 1.0) M H₂SO₄ i.e. the concentration ratio of H₂SO₄ to HCl was maintained 1:1, 10:1, 10²:1 and 10³: 1; depending on the concentration of HCl. The time taken for the attainment of the steady-state potential was maximum for 1.0 M HCl + 1.0 M H₂SO₄ (80 min), whereas in all other cases, it was achieved within 60 min (Fig. 1[b]). Typical results were obtained depending on the molar ratio of both the acids. At equimolar concentration (1:1 ratio), the steady-state potentials shifted to more negative values as compared to the corresponding sulphuric acid-free methanol-HCl solutions. The difference of OCP between such solutions was maximum for 1.0 M concentration of each acid (100 mV) and was limited to only 5 - 10 mV for lower concentrations of each acid (0.001 M), showing the aggressiveness of the acids at high concentration. However, for molar ratio \geq 10:1, the open-circuit potential shifted marginally in the noble direction (with few exceptions). This positive shift was most likely due to the beneficial role of water molecules inherent in sulphuric acid whose concentration increased with H₂SO₄ concentration.

3.2. Polarization measurements

3.2.1. Methanol-HCl

Figure 2 shows the potentiostatic cathodic and anodic polarization curves of the steel in different concentrations of HCl (0.001 – 1.0 M) in methanol. The cathodic polarization curves were associated with well defined Tafel regions with Tafel slopes (b_c) between 120 and 150 mV/dec. Evolution of a gas was also observed on the surface of the electrode. Therefore, the cathodic reaction was considered to be the hydrogen evolution reaction, the predominant reaction in acidic solutions. At low concentrations of hydrochloric acid (0.001 and 0.01 M), the cathodic curves displayed a limiting diffusion current well within a potential region from -500 to -1000 mV. The limiting current values were 1.5×10^2 and 2.0×10^3 $\mu\text{A}/\text{cm}^2$ for 0.001 and 0.01 M HCl, respectively. The appearance of limiting currents in these solutions is most likely due to the lower concentration of H⁺ ion in the solution.

The anodic polarization curves showed only active dissolution due to the presence of aggressive chloride ions and the anodic Tafel slopes (b_a) ranged between 60 and 70 mV/dec. The corrosion parameters are listed in Table 1 which shows that with an increase in the concentration of HCl from 0.001 to 1.0 M, the corrosion potential (E_{corr}) shifted to active potential region and consequently the corrosion current density (i_{corr}) increased significantly. Such behaviour is due to two synergistic effects i.e. increase in aggressiveness of chloride ions as well as the increase in acidity of the solution. Similar results have been reported for aluminium in HCl and H₂SO₄ solutions [7].

The nature of the anodic polarization curves was almost similar where the current density increased rapidly from the corrosion potential (E_{corr}), but beyond a potential of 200 mV, the increase was very steady, resulting in a limiting diffusion current region (except in 1.0 M). This is most likely due to the precipitation of metal chlorides on the surface of the alloy [8]. These corrosion products

(metal chlorides) are loosely bound and are salt-like in nature which act as a barrier for the metal ions entering into the solution and in turn retard the rate of anodic dissolution.

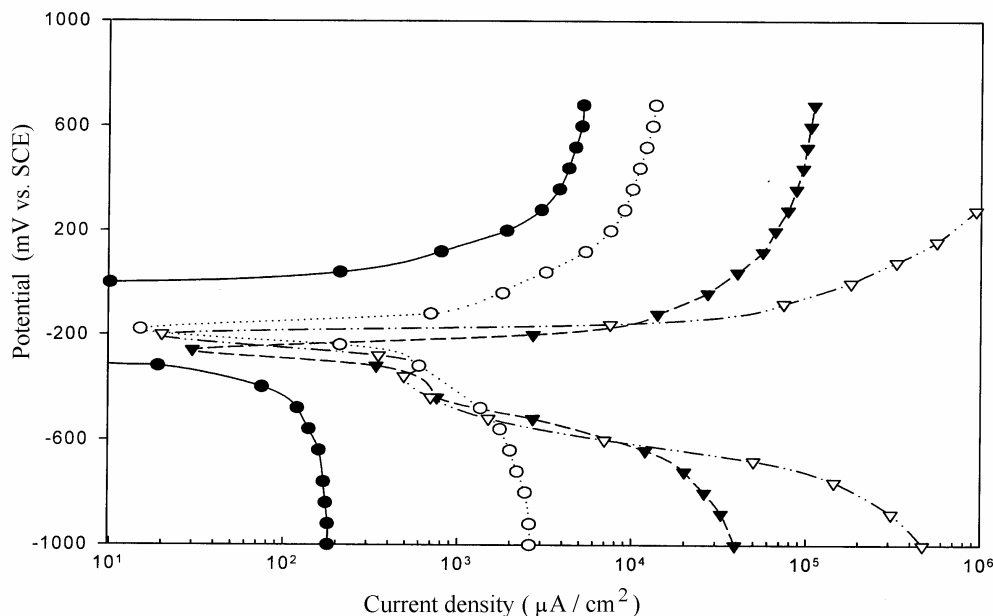


Figure 2. Polarization curves of AISI 304 austenitic stainless steel in different concentrations of HCl in methanol at 35°C. (i) ● 0.001 M HCl, (ii) ○····· 0.01 M HCl, (iii) —▼— 0.1 M HCl, (iv) ···▽··· 1.0 M HCl

After the polarization experiment, the colour of the solution changed to yellow or green depending on the concentration of hydrochloric acid. Also, the colour of the solution intensified with increase in the potential as well as concentration of the acid. Spectral analysis showed the presence of Fe^{3+} and Cr^{3+} ions in the solution owing to their yellow and green colours, respectively.

Table 1. Corrosion parameters of AISI 304 austenitic stainless steel in different concentrations of HCl in methanol at 35°C.

Conc. of HCl (M)	E_{corr} (mV)	$i_{\text{corr.}}$ ($\mu\text{A}/\text{cm}^2$)	b_c (mV/dec)	b_a (mV/dec)
0.001	-170	0.50	140	70
0.01	-190	195	120	70
0.1	-260	200	130	60
1.0	-270	270	120	60

3.2.2. Methanol-HCl + H₂SO₄

Figures 3(a) and 3(b) illustrate the effect of addition of sulphuric acid on the polarization curves of the steel in different concentrations of HCl in methanol. The cathodic polarization curves were almost similar in nature to those observed in case of methanol-HCl solutions and the Tafel slopes (b_c) ranged between 95 and 150 mV/dec. Gas evolution was also observed as in the case of methanol-HCl system in the cathodic potential region indicating hydrogen evolution as the cathodic reaction.

The anodic polarization curves were associated with well-defined Tafel regions where the Tafel slopes (b_a) ranged between 30 and 70 mV/dec. The corrosion parameters are listed in Table 2. When the molar ratio of HCl and H₂SO₄ was 1:1, the steel dissolved actively as was observed in the case of methanol-HCl solution. Moreover, the corrosion current density (*i*_{corr}) was found to be larger and the corrosion potential (*E*_{corr}) shifted to more active values than the corresponding sulphuric acid-free methanol-HCl solution. This indicates that the rate of corrosion is very high in presence of both the acids due to their combined activating effects. At more positive potentials, limiting currents were observed which suggested the growth of a salt film on the electrode surface by precipitation mechanism.

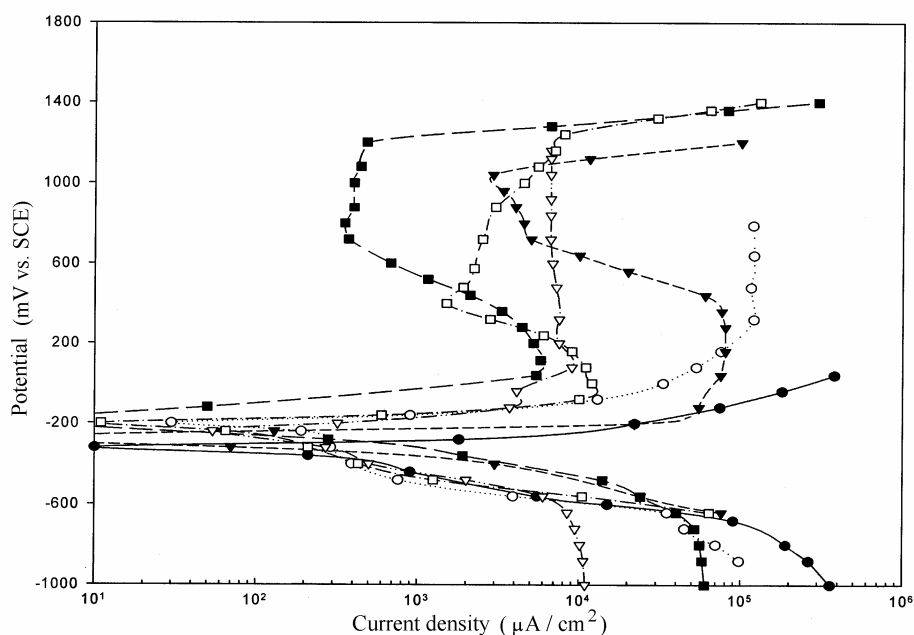


Figure 3(a). Polarization curves of AISI 304 austenitic stainless steel in different composition mixtures of HCl and H₂SO₄ in methanol at 35°C. (i) -▽- 0.01 M HCl + 0.01 M H₂SO₄, (ii) -■- 0.01 M HCl + 0.1 M H₂SO₄, (iii) -□- 0.01 M HCl + 1.0 M H₂SO₄, (iv) ···· O··· 0.1 M HCl + 0.1 M H₂SO₄, (v) -▼- 0.1 M HCl + 1.0 M H₂SO₄, (vi) ● 1.0 M HCl + 1.0 M H₂SO₄

Probably the precipitated salt was composed of FeSO₄ and FeCl₂ [9], because iron was the main constituent of the steel. Moreover, the limiting currents are more pronounced in solutions containing less amounts of acids (0.001 and 0.01 M) which indicate that the salt film is more stable in solutions of lower acidity.

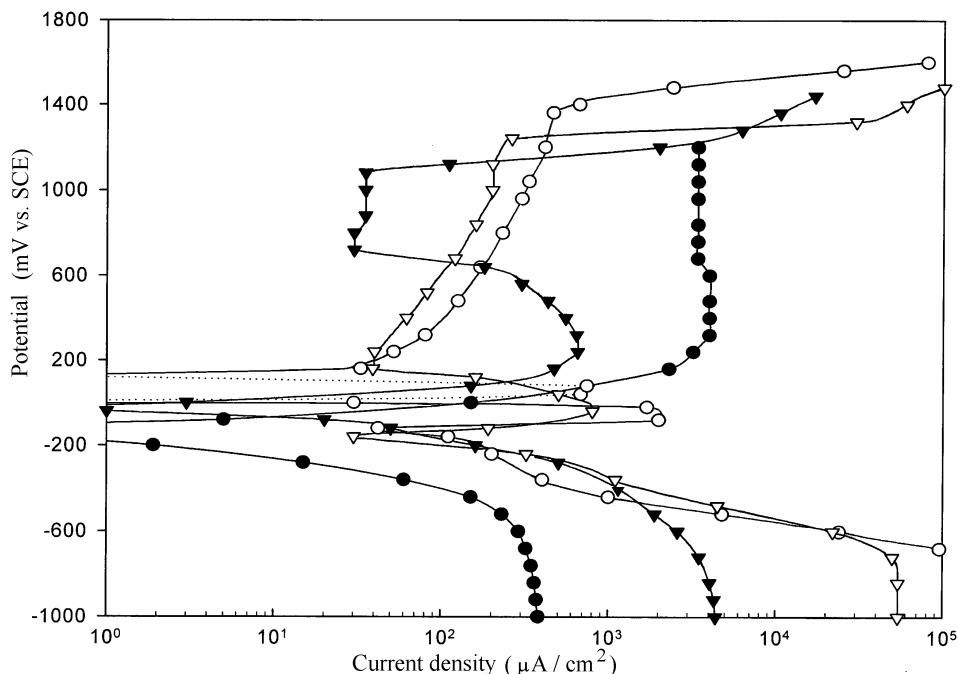


Figure 3(b). Polarization curves of AISI 304 austenitic stainless steel in different composition mixtures of HCl and H₂SO₄ in methanol at 35°C. (i) • 0.001 M HCl + 0.001 M H₂SO₄, (ii) --▼-- 0.001 M HCl + 0.01 M H₂SO₄, (iii) ···▼··· 0.001 M HCl + 0.1 M H₂SO₄, (iv) ···○··· 0.001 M HCl + 1.0 M H₂SO₄

When the concentration of H₂SO₄ to HCl approached 10²:1, 10³:1, the polarization curves revealed active, passive and transpassive behaviour with the occurrence of pitting on the electrode surface. As compared to ratio 1:1, the i_{corr} decreased for ratio 10:1 (except in 0.001 M HCl solution), but it again increased considerably when the molar ratio approached 10²:1 and 10³:1. The critical current density for passivation (i_{crit}) also increased in the order 10:1 < 10²:1 < 10³:1. Since the concentration of H₂SO₄ was significantly higher than that of HCl, the predominant corrosion product formed in the active region seems to be the soluble metal sulphates. Therefore, an increase in sulphuric acid concentration for a particular HCl concentration increased the rate of metal dissolution significantly in the active region. However, in the case of 0.001 M HCl + 1.0 M H₂SO₄ solution, negative currents were observed in the anodic potential region up to potential 160 mV (dashed line in Figure 3[b]). The negative current observed in anodic region is considered as “cathodic loop” and has been reported by several authors [10-12]. According to them, the cathodic loop appears either due to hydrogen evolution or due to the reduction of oxygen even in helium saturated solution. In the present case, it may be due to either of the two reasons or both.

For H₂SO₄ to HCl concentration ratio 10:1, the active to passive transition region was quite broad and the range of passivity ($E_{\text{pit}} \sim E_{\text{pass}}$) was narrow showing feeble passivating effect. Increasing this ratio to 10²:1 and 10³:1 shifted the passivation potential (E_{pass}) to a more active region and the transpassive potential to noble direction thereby broadening the range of passivity (Table 2). At the same time, the passivation current density (i_p) increased in the order 10:1 < 10²:1 < 10³:1. Since the current density in the passive range was not constant and increased gradually with potential, the reported values of i_p were calculated by taking the average of the current values in this region. The

higher i_p value indicates that the passive film becomes relatively more unstable with increase in the concentration of H_2SO_4 for a particular HCl concentration. Particularly, in 0.01 M HCl + 1.0 M H_2SO_4 , the large i_p value accompanied with very high i_{crit} reflects the less protective nature of the film on the surface.

Table 2. Corrosion parameters of AISI 304 austenitic stainless steel in different composition mixtures of HCl and H_2SO_4 in methanol at 35°C.

Conc. of HCl (M)	Conc. of H_2SO_4 (M)	E_{corr} (mV)	i_{corr} ($\mu A/cm^2$)	i_{crit} ($\mu A/cm^2$)	i_p ($\mu A/cm^2$)	E_{pass} (mV)	E_{pit} (mV)	$(E_{pit} \sim E_{pass})$ (mV)
0.001	0.001	-180	1.5	-	-	-	-	-
0.001	0.01	0	3.6	650	33	720	1080	360
0.001	0.1	-150	47	850	76	160	1240	1080
0.001	1.0	-100	55	2000	181	160	1360	1200
0.01	0.01	-280	200	-	-	-	-	-
0.01	0.1	-150	18	5500	410	720	1200	480
0.01	1.0	-200	27	12000	4700	400	1240	840
0.1	0.1	-280	235	-	-	-	-	-
0.1	1.0	-270	77	75000	3900	720	1040	320
1.0	1.0	-370	285	-	-	-	-	-

The onset of passivity in solutions containing H_2SO_4 to HCl molar ratio $\geq 10:1$ is most likely due to the inherent water content of sulphuric acid. Beneficial role of water molecules on the onset and stability of the passive films has been reported earlier also [13-15]. For the formation of passive film, a certain minimum concentration of water is required and is termed as 'critical water concentration' which varies from material to material. In this case, the water content of the solutions seems to be certainly higher than the critical water concentration required for passivation. For a particular HCl concentration, when the concentration of H_2SO_4 increased, the water content of the respective solution increased appreciably which in turn enhanced passivation, characterized by broadening of the passivation range and shifting of the pitting potential (E_{pit}) in the noble direction. It appears that the ratio of H_2SO_4 to HCl also plays a significant role for the onset of passivity in this system and the ratio should be nearly $\geq 10:1$; as it is apparent that at equal concentration (1:1), only active anodic dissolution occurred in spite of the presence of higher water content in the solutions. The shifting of the pitting potential (E_{pit}) to noble direction can also be related with the inhibition effect of sulphate ions (SO_4^{2-}) against chloride induced pitting [16, 17]. The passive film formed on the stainless steel in sulphuric acid solution appears to have a bilayer structure, the inner chromium rich oxyhydroxide layer and the outer layer, rich in iron [18, 19]. The outer iron rich layer incorporates the anion of the electrolyte, as a consequence, a coulombic barrier against anion adsorption is formed which offers resistance against pitting. In the present case, the passive film can be considered to be of the bilayer structure and sulphate ion is expected to be incorporated into it. Since higher passivation currents (i_p) are observed for higher H_2SO_4 concentration, it is reasonable to assume that a more defective passive film is being formed probably due to the higher acidity of the respective solutions. Thus the sulphate

ion can more easily enter into it and as a result the sulphate content of the film increases. The sulphate ions then inhibit the ingress of aggressive chlorides ions effectively resulting in enhanced resistance against pitting.

3.3. Cyclic anodic polarization and i vs. t measurements

Figures 4(a) and 4(b) represent the cyclic anodic polarization curves for the steel in different concentration ratios of H_2SO_4 and HCl in methanol. At ratio 10:1, the pitting potential (E_{pit}) was observed at 1200 mV (for 0.001 M HCl + 0.01 M H_2SO_4). E_{pit} was characterized by a sharp and continued increase in current with applied potential. Increasing the molar ratio to $10^2:1$ and $10^3:1$, the E_{pit} shifted to more positive direction. Similar results were also observed for the protection potential (E_{prot}) i.e. the potential at which the descending curve during the reverse scan intersected the ascending curve; at zero current value in the present case. This can be due to the enhanced passivity in the presence of higher water content of the solutions. Also, the preferential adsorption of SO_4^{2-} ions on the passive film increases with increase in H_2SO_4 concentration which limits the chloride adsorption and thus shifts the E_{pit} in noble direction. Contrary to this, the anodic current also increased indicating intense pitting attack. This can be explained as follows: the sulphate ion gets preferentially adsorbed on the passive film thereby limiting the chloride ingress and hence inhibits the initiation of pitting. At the same time, the passive film becomes more defective due to the incorporation of sulphate ions. Thus, chloride ions can enter into the passive film more easily than before favouring intense pitting attack [20].

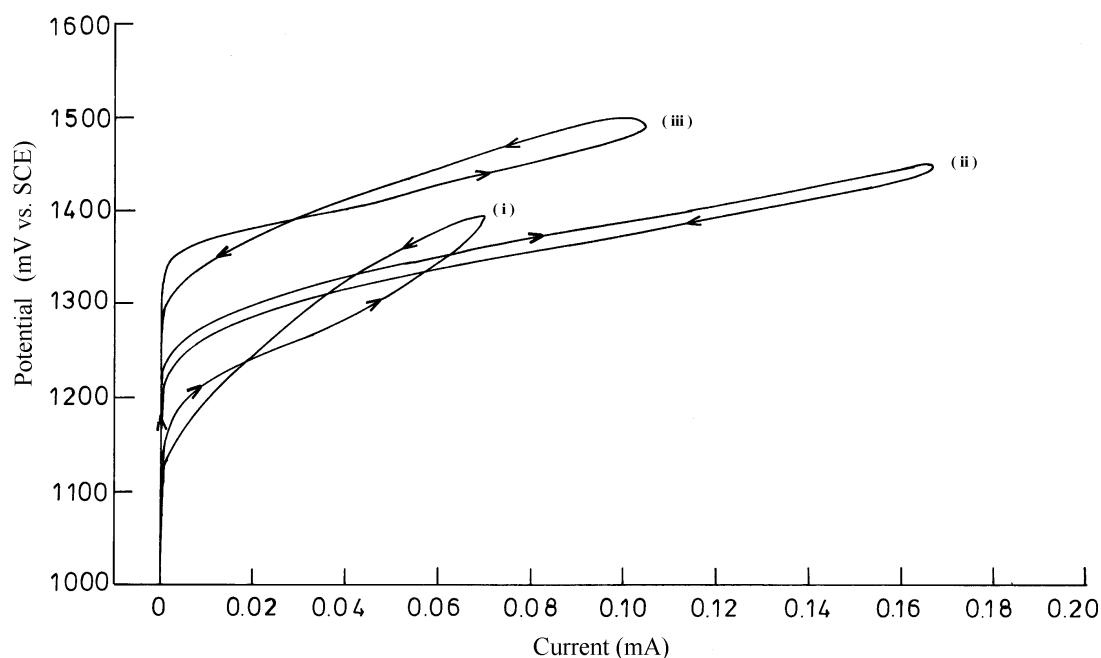


Figure 4(a). Cyclic anodic polarization curves of AISI 304 austenitic stainless steel in different composition mixtures of HCl and H_2SO_4 in methanol at 35°C . (i) 0.001 M HCl + 0.01 M H_2SO_4 , (ii) 0.001 M HCl + 0.1 M H_2SO_4 , (iii) 0.001 M HCl + 1.0 M H_2SO_4

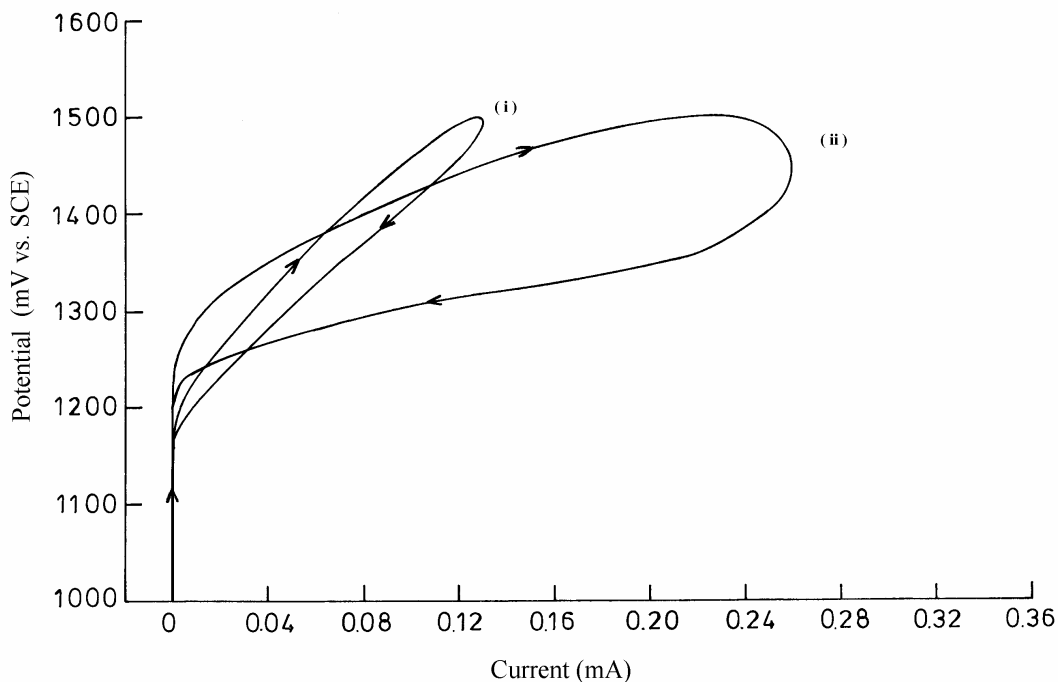


Figure 4(b). Cyclic anodic polarization curves of AISI 304 austenitic stainless steel in different composition mixtures of HCl and H₂SO₄ in methanol at 35°C. (i) 0.01 M HCl + 0.1 M H₂SO₄, (ii) 0.01 M HCl + 1.0 M H₂SO₄

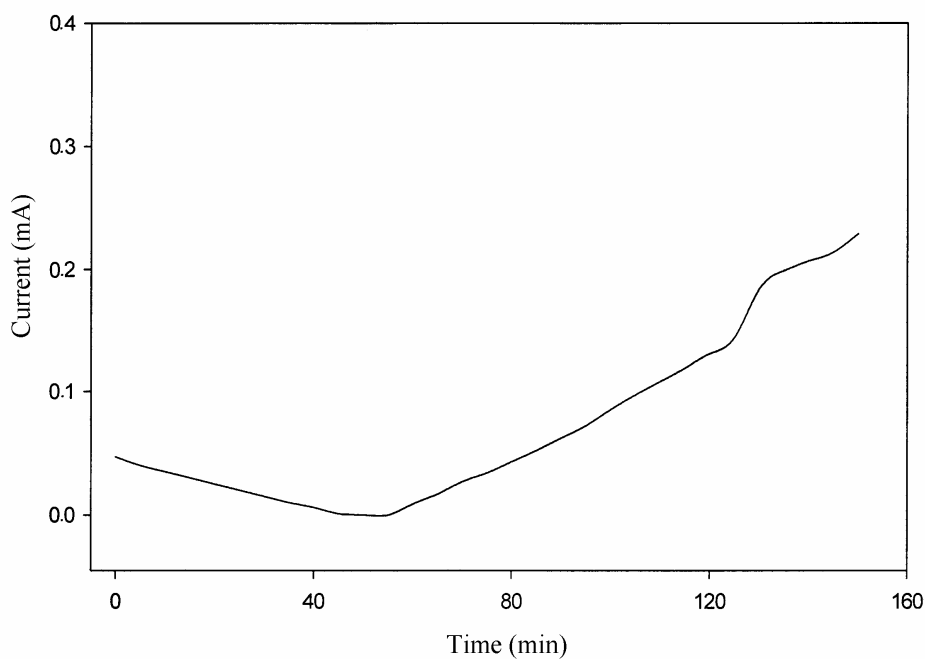


Figure 4(c). Current vs. time plot of AISI 304 austenitic stainless steel in 0.001 M HCl + 1.0 M H₂SO₄ in methanol at 35°C.

The current versus time transient of the steel in 0.001 M HCl + 1.0 M H₂SO₄ (Figure 4[c]) shows that after initial decrease, the current increased continuously with time at potential closer to the

pitting potential (E_{pit}). The continuous increase of current is due to the propagation of the already nucleated pits to form stable pits.

3.4. SEM studies

Figure 5(a) shows the scanning electron micrograph of AISI 304 austenitic stainless steel after polarization studies in 0.01 M HCl solution of methanol, where dissolution proceeds preferentially along the grain boundaries. This may be due to the presence of inclusions such as carbides. Similar results have been reported earlier in hydrochloric acid solutions [21].

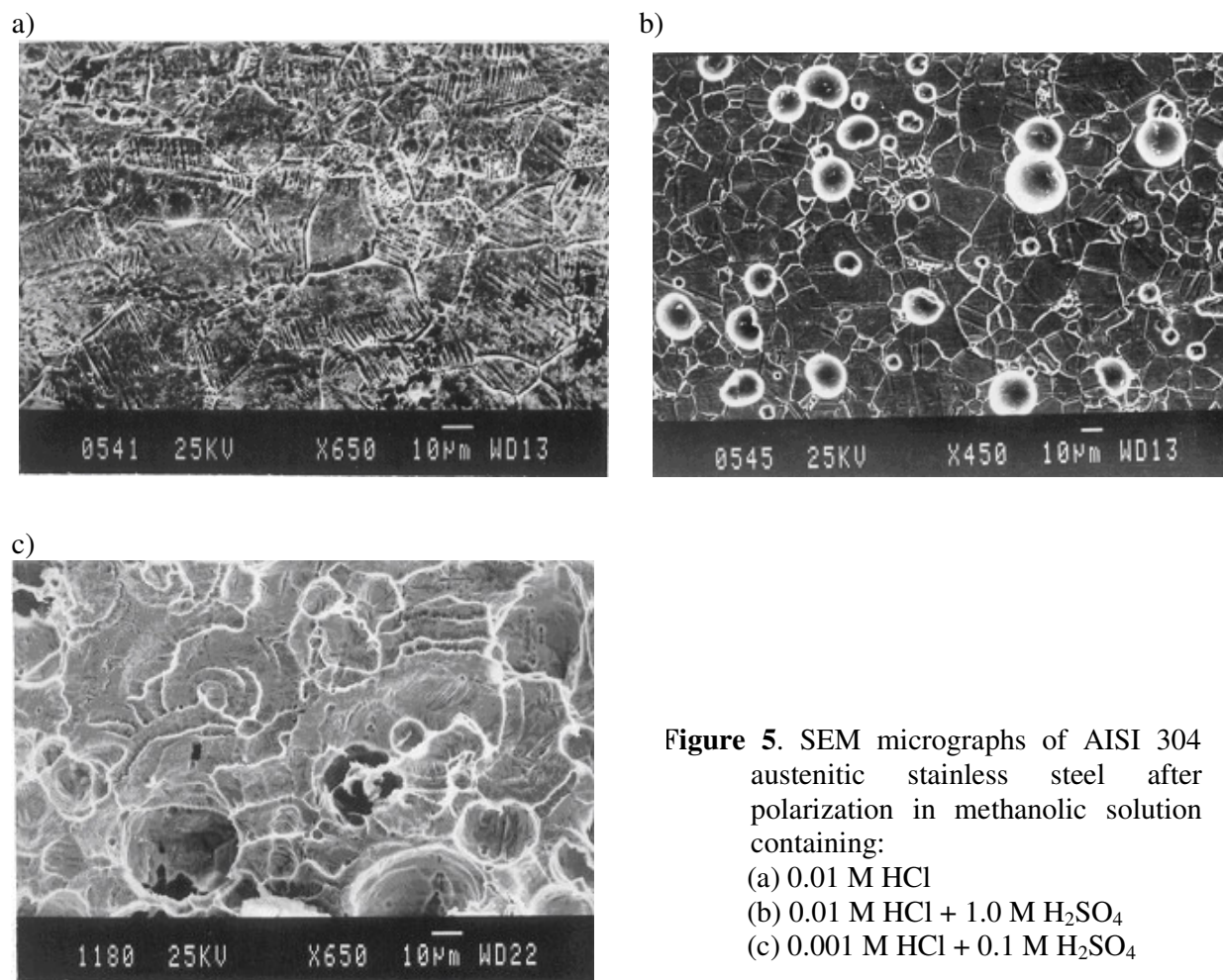


Figure 5. SEM micrographs of AISI 304 austenitic stainless steel after polarization in methanolic solution containing:
(a) 0.01 M HCl
(b) 0.01 M HCl + 1.0 M H₂SO₄
(c) 0.001 M HCl + 0.1 M H₂SO₄

Figure 5(b) shows the micrograph in 0.01 M HCl + 1.0 M H₂SO₄ solution which reveals typical pitting attack on the surface. The pits are shallow, spherical in shape and are dispersed randomly and frequently on grain boundaries. The pits seem to be covered type with the accumulation of corrosion products at the periphery. The SEM micrograph (Figure 5(c)) in 0.001 M HCl + 0.1 M H₂SO₄ solution shows that the surface is covered by some film which has the tendency of pitting.

4. CONCLUSIONS

1. In methanol-HCl solution, the AISI 304 austenitic stainless steel dissolves actively and the rate of corrosion increases with concentration of HCl. The steel suffers from grain boundary attack.
2. The water content of the solution seems to govern the active-passive behaviour.
3. The addition of H₂SO₄ into methanol-HCl solution modifies the corrosion behaviour and concentration ratio of H₂SO₄ to HCl \geq 10:1 facilitates the process of passivation. The steel suffers from pitting and the sulphate ion (SO₄²⁻) shows inhibiting effect against the aggressive chloride ions responsible for pitting.

ACKNOWLEDGEMENTS

Financial assistance provided by Council of Scientific and Industrial Research (CSIR), New Delhi, India is gratefully acknowledged.

References:

1. J. Banas, B. Mazurkiewicz and B. Stypula, *Electrochimica Acta*, 37 (1992) 1069.
2. V. B. Singh and B.N. Upadhyaya, *Corrosion Science*, 40 (1998) 705.
3. J. R. Kish, M. B. Ives and J. R. Rodda, *Corrosion Science*, 45 (2003) 1571.
4. B. Stypula and J. Banas, *Electrochimica Acta*, 38 (1993) 2309.
5. V. K. Singh and V. B. Singh, *Corrosion Science*, 28 (1988) 385.
6. W. A. Badawy, K. M. Ismail and A. M. Fathi, *Electrochimica Acta*, 50 (2005) 3603.
7. S. I. Pyun, K. H. Na, W. J. Lee and J. I. Park, *Corrosion*, 56 (2000) 1015.
8. P. C. Pistorius and G. T. Burstein, *Corrosion Science*, 33 (1992) 1885.
9. J. Flis and M. Kuczynska, *J. Electrochemical Society*, 151 (2004) B 573.
10. I. L. Rozenfeld, *Corrosion*, 37 (1981) 371.
11. N. D. Greene, *J. Electrochemical Society*, 107 (1960) 4571.
12. R. P. Frankenthal, *J. Electrochemical Society*, 114 (1967) 542.
13. Z. Szklarska – Smialowska and J. Mankowski, *Corrosion Science*, 22 (1982) 1105.
14. R. Umehayashi, N. Akao, N. Hara and K. Sugimoto, *J. Electrochemical Society*, 150 (2003)B295.
15. M. Sakakibara, N. Saito, H. Nishihara and K. Aramaki, *Corrosion Science*, 34 (1993) 391.
16. R. M. Carranza and M. G. Alvarez, *Corrosion Science*, 38 (1996) 909.
17. H. P. Leckie and H. H. Uhlig, *J. Electrochemical Society*, 113 (1966) 12.
18. S. Virtanen, E. M. Moser and H. Bohni, *Corrosion Science*, 36 (1994) 373.
19. A. Barbucci, G. Cerisola and P. L. Cabot, *J. Electrochemical Society*, 149 (2002) B 534.
20. A. H. Moreira, A. V. Benedetti, P. T. A. Sumodjo, J.A. Garrido and P. L. Cabot, *Electrochimica Acta*, 47 (2002) 2823.
21. P. L. Cabot, F. A. Centellas, J. A. Garrido, E. Perez and H. Vidal, *Electrochimica Acta*, 36 (1991) 179.